SCIENCE CHINA
Information Sciences

• RESEARCH PAPER •

August 2017, Vol. 60 082301:1–082301:12
doi: 10.1007/s11432-016-0097-4

A high-precision phase-derived range and velocity measurement method based on synthetic wideband pulse Doppler radar

Huayu FAN[1,2], Lixiang REN[1,2*], Teng LONG[1,2] & Erke MAO[1,2]

[1]*Beijing Key Laboratory of Embedded Real-time Information Processing Technology, Beijing Institute of Technology, Beijing* 100081*, China;*
[2]*Radar Research Laboratory, Beijing Institute of Technology, Beijing* 100081*, China*

Received June 30, 2016; accepted August 3, 2016; published online December 8, 2016

Abstract Development of radar technology needs to address the two-dimensional high resolution of range and velocity simultaneously for high-speed targets. Taking advantage of the superior coherent performance of synthetic wideband pulse Doppler radar, this paper elaborates the principles of phase-derived range and velocity measurements. Moreover, this paper explores the key technologies of unwrapping phase ambiguity, and discusses the phase unwrapping strategy at a low signal-to-noise ratio (SNR). The proposed method can be applied to the conditions of low SNR and has comparatively strong practicality in engineering. Both the ejection ball and civil aircraft experiments have validated the correctness and feasibility of the proposed method. In particular, the experimental results reveal that the accuracy of phase-derived range and velocity measurement has reached a level of submillimeter or millimeter and centimeter/second or submillimeter/second, respectively.

Keywords synthetic wideband PD radar, phase-derived range measurement, phase-derived velocity measurement, unwrapping phase ambiguity, track filtering, minimum entropy method

Citation Fan H Y, Ren L X, Long T, et al. A high-precision phase-derived range and velocity measurement method based on synthetic wideband pulse Doppler radar. Sci China Inf Sci, 2017, 60(8): 082301, doi: 10.1007/s11432-016-0097-4

1 Introduction

Application demands on high-precision range and velocity measurements of targets have been increasing in a variety of fields, such as micromotion measurements, target identification, precision guiding, etc. Fortunately, the continuous advancement of radar technology has also provided further space for the development of accurate radar measurements.

According to the theory of radar systems, in order to improve the precision of radar velocity measurements, the length of coherent processing time must be increased, whereas increasing the signal bandwidth is required to improve the precision of range measurements. With respect to high-speed targets, it is generally difficult to balance long-time coherent accumulation and large signal bandwidths. This is because the large bandwidth of the signal is restricted to a very narrow pulse in the time domain after

* Corresponding author (email: lixiangr@bit.edu.cn)

matched filtering. If the target has a high velocity, and thus the range migration of the target within the coherent processing time is greater than the main lobe width of the narrow time domain pulse after matched pulse compression, it is unable to achieve an effective accumulation of coherent pulse trains. Synthetic wideband pulse Doppler (PD) radar adopts instantaneous narrowband and synthetic wideband signals. This occurs by, first, performing the PD process on the narrowband subpulses at different frequencies to distinguish the target and clutter from the velocity dimension, and then conducting a synthetic pulse compression process from the velocity dimension, where the target is located to gain high-resolution range-velocity imaging of the target, thereby achieving a coherent accumulation of the target echo from the dimensions of range and velocity [1]. Typical synthetic wideband PD radar signals consist of a stepped-frequency (SF) signal [2], a stepped-frequency chirp (SFC) signal [3, 4], intra-pulse phase encoding, inter-pulse stepped-frequency (PCSF) signal [5], in addition to others.

In this paper, enabled by the motion stability of the target and good coherent performance of the synthetic wideband PD radar, a phase-derived range and velocity measurement method with high precision at a low signal-to-noise ratio (SNR) has been proposed. This paper is organized as follows. First, it introduces the basic principles of the phase-derived range measurement and analyzes its theoretical precision. Then, it describes the process flow of the phase-derived range and velocity measurement based on synthetic wideband PD radar, highlights the implementation principles of the phase-derived range and velocity measurement with high precision, and proposes a method of correctly unwrapping the phase ambiguity at low SNR. Finally, both the ejection ball and civil aircraft experiments based on a dominant scatterer have verified the correctness and feasibility of this method. The experimental results show that the accuracy of the phase-derived range measurement has reached a level of submillimeter or millimeter, and the accuracy of phase-derived velocity measurement has reached a level of centimeter/second or submillimeter/second, which are consistent with the theoretical analysis results.

2 Phase-derived range measurement method

2.1 Basic principles of phase-derived range measurement

The target range R and echo phase Φ satisfy the following relationship:

$$R = \frac{\lambda}{4\pi}\Phi, \tag{1}$$

where λ signifies the signal wavelength. From the above equation, the phase of the radar echo varies depending on the target range. When the target moves radically by half the wavelength, the echo phase changes by 2π. The range measurement method through the change in the echo phase is referred to as the phase-derived range measurement [6, 7].

In general, the target range is much greater than a half wavelength, i.e., the echo phase is subject to ambiguity:

$$\Phi = 2\pi K + \Delta, \tag{2}$$

where $\Delta(0 \leqslant \Delta < 2\pi)$ is the ambiguity phase, and K is the phase ambiguity number. The key of the phase-derived range measurement is to unwrap the phase ambiguity number K.

After obtaining high precision ranging results, the application of the range change rate for velocity measurements can achieve high-precision velocity measurement results.

2.2 Precision analysis of phase-derived range measurement

According to the principles of radar, the range measurement can utilize the radar echo envelope delay, and its theoretical root mean square error (RMSE) is expressed as follows [8]:

$$\delta_{\text{Env\_}R} = \frac{ct_r}{2(S/N)^{1/2}}, \tag{3}$$

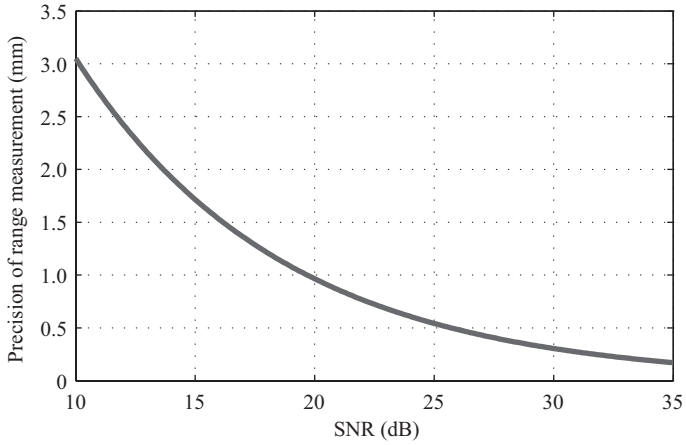

Figure 1 Precision of the phase-derived range measurement at different SNRs.

where t_r is the rise time of the output echo after matched filtering, $t_r = 1/\beta$, β is the effective bandwidth of the signal, and S/N is the signal to noise ratio. B is assumed to be a half-power bandwidth for quasi-rectangular pulse; therefore, $\beta = 2.38B$.

The error equation of the phase measurement for radar is written as

$$\delta_{\text{Pha\_}\varphi} = \frac{1}{(2S/N)^{1/2}}. \tag{4}$$

The above equation was converted to the corresponding error of the phase-derived range measurement ($\delta_{\text{Pha\_}R}$), and then the precision between envelope range measurement and phase-derived range measurement was compared:

$$\frac{\delta_{\text{Pha\_}R}}{\delta_{\text{Env\_}R}} = \frac{\beta}{\sqrt{2}\cdot 2\pi f_{\text{c}}} = \frac{2.38B}{\sqrt{2}\cdot 2\pi f_{\text{c}}} = 0.27k_B, \tag{5}$$

where f_{c} is the carrier frequency of the signal, and $k_B = B/f_{\text{c}}$ is the relative bandwidth of the signal. Let $k_B = 0.1$, then $\delta_{\text{Pha\_}R}/\delta_{\text{Env\_}R} = 0.027$, and, thus, the error of the phase-derived range measurement will be 2.7% of that by the envelope range measurement.

Figure 1 shows the theoretical precision of the phase-derived range measurement at different SNRs, wherein the center frequency of the signal is 3.5 GHz. It is indicated that when the SNR is 10–35 dB, the RMSE of the range measurement reaches the level of submillimeter or millimeter.

3 A phase-derived range and velocity measurement method based on synthetic wideband PD radar

Synthetic wideband PD radar is capable of attaining the coherent accumulation of target echoes from the dimensions of range and velocity [1]. By enabling motion stability of the target and good coherent performance for the synthetic wideband PD radar [9], a phase-derived range and velocity measurement method with high precision based on synthetic wideband PD radar has been proposed through theoretical research and a large number of engineering experiments. The process flow of this method is shown in Figure 2.

In accordance with this process, the phase-derived range and velocity measurement method based on the synthetic wideband PD radar mainly consists of the following implementation steps:

(1) Static and low-speed heavy clutter needs to be filtered out. Then, Doppler processing at the same frequency for M synthetic wideband echo frames is performed, target and clutter is distinguished from the velocity dimension, static or low-speed clutter near zero frequency is filtered. Thus, the remaining information is for the moving target, from which the time-domain waveform is recovered by IFFT transformation, significantly improving the echo SNR [3].

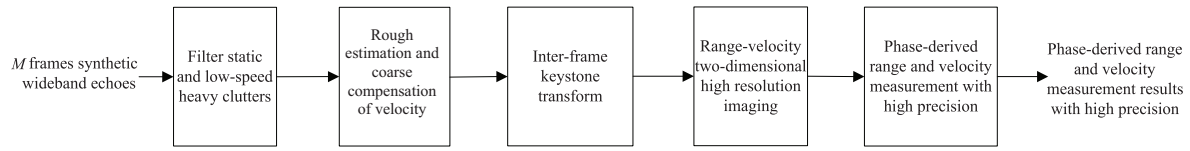

Figure 2 Process flowchart of the phase-derived range and velocity measurement based on the synthetic wideband PD radar.

(2) If the velocity of the target is high, Doppler processing at the same frequency is restricted by velocity ambiguity. Thus, it needs to conduct a rough estimation and coarse compensation for the velocity of the echo. The rough estimate of the velocity can use a moving target velocity estimation method based on the Doppler frequency difference [10], which first performs inter-frame PD process for the echo, and then employs a Hough transformation to gain the Doppler frequency difference between different carrier frequencies to estimate the motion velocity of the target.

(3) With regard to the high-resolution process for the synthetic wideband PD radar signal, due to the disparity in the carrier frequencies of the narrowband subpulses, it is subject to a Doppler spreading effect [3], resulting in amplitude heterogeneity and phase nonlinearity of various subpulses, the presence of incomplete accumulation, etc. Thus, it is capable of eliminating the impact of slow time-domain-coupled phase terms via Keystone transformation [1, 11, 12].

(4) The inter-frame PD process for the echo after Keystone transformation is performed, the moving target is distinguished from the velocity dimension, and coherent synthetic pulse compression for the targets at different velocity channels is executed to obtain the range-velocity high-resolution imaging results.

(5) The one-dimensional high-resolution range profile (HRRP) of the velocity dimension is selected, where the target located, and the phase-derived range and velocity measurement process is implemented to obtain the final high-precision range and velocity measurement results.

Subsequently, we will elaborate the key steps of the above-mentioned flowchart, mainly including the echo signal modeling, two-dimensional range-velocity high-resolution imaging, and high-precision phase-derived range and velocity measurement process.

3.1 Echo signal modeling

The synthetic wideband PD radar signals (e.g., the SFC and PCSF signals) can be equivalent to SF signals after matched subpulse compression. The following section will take the SF signal as an example to conduct signal modeling, and the subsequent signal processing algorithms are established in this model. The single-frame echo signal at a scattering point of the target with a range of R is written as

$$s(t) = \sum_{n=0}^{N-1} \mathrm{rect}\left(\frac{t - nT_r - \frac{\tau}{2} - \frac{2R}{c}}{T_r}\right) \exp\left[-\mathrm{j}2\pi(f_0 + n\Delta f)\frac{2R}{c}\right], \tag{6}$$

where t refers to the fast time, τ signifies pulse width, T_r represents the repetition period of a single sub-pulse, f_0 indicates the initial carrier frequency, Δf represents the frequency stepping size, N refers to the number of frequency stepping pulses, and c signifies the velocity of light.

If the radar receives M echo frames, considering that the initial range and velocity of the target are R_0 and v, then the instantaneous range of the target at each interval of T_r will be $R_{m,n} = R_0 - (mNT_r + nT_r)v$, $m = 1, 2, \ldots, M$, such that the mth echo frame is

$$s_m(t) = \mathrm{rect}\left(\frac{t - \frac{\tau}{2} - nT_r - mNT_r - \frac{2R_{m,n}}{c}}{\tau}\right) \cdot \exp\left[-\mathrm{j}2\pi(f_0 + n\Delta f)\frac{2R_{m,n}}{c}\right]. \tag{7}$$

3.2 Two-dimensional range-velocity high-resolution imaging

The focus of this paper is to discuss the high-precision range and velocity measurement method, and thus it neither models the clutter nor takes the rough estimation and coarse compensation process of the

velocity into account. The following section presents the range-velocity high-resolution imaging results via Keystone transformation, and then obtains the one-dimensional HRRPs of the velocity dimension where the target is located, which are used for the subsequent high-precision phase-derived range and velocity measurement process.

When the velocity of the target is high, the synthetic wideband PD radar signal is restricted by the Doppler spreading effects, which can be eliminated through Keystone transformation, i.e., achieving resampling through the nonlinear transformation (compression and broadening) of the slow time $t_m = mNT_r$ such that the product of $f_n = f_0 + n\Delta f$ and $t_m = mNT_r$ is a constant [11].

To eliminate the impact of the slow time-domain coupled phase terms, we need to find a new sampling interval that satisfies the conditions below:

$$(f_0 + n\Delta f)\, mNT_r = f_0 m_k NT_r. \tag{8}$$

Substituting (8) into (7) and ignoring the echo envelope, we can obtain an expression of the echo after the Keystone transformation:

$$s'(m_k, n) = \exp\left(\mathrm{j}2\pi f_0 \frac{2v \cdot m_k NT_r}{c}\right) \cdot \exp\left[-\mathrm{j}2\pi\left(f_0 + n\Delta f\right)\frac{2\left(R_0 - v \cdot nT_r\right)}{c}\right]. \tag{9}$$

The above equation is a function of the delay and Doppler frequency. It has been suggested that this eliminated the impact of the moving object walking across Doppler resolution cells in the coherent processing time after the Keystone transformation.

Assume $f_{d0} = 2vf_0/c$, $f_{\mathrm{c}} = f_0 + (N-1)\,\Delta f/2$, by virtue of the longitudinal Doppler velocity measurement and transverse IFFT coherent pulse compression imaging process on Eq. (9), it can derive the amplitude term of the range-velocity after the two-dimensional pulse compression:

$$|I_k(k,l)| = \left|\frac{\sin\left[\pi\left(f_{d0}NT_r - N\Delta f\frac{2R_0}{c} + l\right)\right]}{\sin\left[\frac{\pi}{N}\left(f_{d0}NT_r - N\Delta f\frac{2R_0}{c} + l\right)\right]}\right| \left|\frac{\sin\left[\pi\left(f_{d0}MNT_r - k\right)\right]}{\sin\left[\frac{\pi}{M}\left(f_{d0}MNT_r - k\right)\right]}\right|. \tag{10}$$

The phase term is written as follows:

$$\begin{aligned}\arg\left[I_k(k,l)\right] = &-2\pi f_{\mathrm{c}}\frac{2R_0}{c} + \pi\frac{N-1}{N}l - \pi\frac{M-1}{M}k \\ &+ \pi\frac{M-1}{M}f_{d0}MNT_r + \pi\frac{N-1}{N}f_{d0}NT_r,\end{aligned} \tag{11}$$

wherein the 1st term reflects the relationship between the target range and phase change, which is the desired phase term, denoted as φ_t; the 2nd term is needed to compensate for the target range changes, denoted as φ_{cmp1}; the 3rd term is needed to compensate for the target velocity changes, denoted as φ_{cmp2}; and the 4th and 5th terms are correlated with the target velocity.

3.3 High-precision phase-derived range and velocity measurement process

In accordance with the range-velocity high-resolution imaging results of the target, we are able to obtain the one-dimensional HRRP of the velocity dimension where the target is located. Eqs. (10) and (11) reveal that the target range is not only in correlation with the peak position of the one-dimensional HRRP, but its envelope and phase also contain the range information. Thus, we can use the envelope information of the one-dimensional HRRP for the envelope range measurement. For example, the waveform analysis method [13] can be used to derive the area center of the cross-correlated output envelope to improve the accuracy of the range measurement. In addition, we can also utilize the phase information of the one-dimensional HRRP for the phase-derived range measurement to further improve its accuracy. However, the phase-derived range measurement results are subject to ambiguity, and the key to implementing the phase-derived range measurement is to correctly unwrap the ambiguity of the range measurement according to the phase.

As we are usually unable to identify the true range of the target and initial phase of the system in reality, we may analyze the amount of change in the ranges and phases of adjacent frames with respect to the process of moving targets [14].

3.3.1 *Phase extraction*

With respect to the one-dimensional HRRPs of two adjacent frames, assume their initial ranges and velocities as R_1, R_2 and v_1, v_2, respectively, and φ_{cmp1} and φ_{cmp2} in (11) have been compensated for

$$\arg\left[I_k(k,l)\right]_1 = -2\pi f_{\text{c}}\frac{2R_1}{c} + \pi\frac{M-1}{M}\frac{2v_1 f_0}{c}MNT_r + \pi\frac{N-1}{N}\frac{2v_1 f_0}{c}NT_r, \tag{12}$$

$$\arg\left[I_k(k,l)\right]_2 = -2\pi f_{\text{c}}\frac{2R_2}{c} + \pi\frac{M-1}{M}\frac{2v_2 f_0}{c}MNT_r + \pi\frac{N-1}{N}\frac{2v_2 f_0}{c}NT_r. \tag{13}$$

Assume $R_2 = R_1 + \Delta R$, $v_2 = v_1 + \Delta v$, subtract (13) from (12), then

$$\Delta\left\{\arg\right\} = -2\pi f_{\text{c}}\frac{2\Delta R}{c} + \pi\frac{M-1}{M}\frac{2\Delta v f_0}{c}MNT_r + \pi\frac{N-1}{N}\frac{2\Delta v f_0}{c}NT_r. \tag{14}$$

In the above equation, the first term is the phase desired term. When the target is moving uniformly, i.e., $\Delta v = 0$, the 2nd and 3rd terms are zero, which will not cause interference. When the target performs variable motion, i.e., $\Delta v \neq 0$, $\Delta R_e = (MN-1)f_0\Delta v T_r/2f_{\text{c}}$, assume that the target undergoes uniformly accelerated motion and its acceleration is a, then $\Delta R_e \approx \Delta v \cdot MNT_r/2 = a \cdot MNT_r \cdot MNT_r/2 = a(MNT_r)^2/2$. It can be understood that here the required range increment is $\Delta R + \Delta R_e \approx vMNT_r + a(MNT_r)^2/2$, then the desired velocity refers to the average velocity during this period, i.e., $\overline{v} = (\Delta R + \Delta R_e)/MNT_r \approx v + aMNT_r/2$.

To sum up, by extracting the phase of the maximum reflection point in the one-dimensional HRRP of the target, and obtaining the phase difference of adjacent frames, for the case of correctly unwrapping the phase ambiguity, we are able to measure the range increment between adjacent frames, and further derive the target velocity (range increment/interval of adjacent frames) and the range change trajectory of the target (integral of range increments over time).

3.3.2 *Unwrapping phase ambiguity strategy*

The essential result of the phase-derived range measurement is to correctly unwrap the phase ambiguity. The commonly used method is to use the unwrapping phase ambiguity by envelope range measurement, which has higher requirements on SNR [6, 7, 15, 16]. To accurately determine the number of phase ambiguities, the absolute value for the maximum tolerance of the envelope range measurement upon being converted to a phase must be less than π radians, i.e., the RMSE is smaller than the $\pi/3$ radians. Converting the envelope range measurement error in (3) into a phase measurement error, it was inferred that the following should be met:

$$\delta_{\text{Env\_}\varphi} = \frac{2\pi f_{\text{c}}}{\beta(S/N)^{1/2}} < \frac{\pi}{3}. \tag{15}$$

Therefore, the SNR must satisfy the conditions given below:

$$\frac{S}{N} > \left(\frac{6f_{\text{c}}}{\beta}\right)^2. \tag{16}$$

If the central carrier frequency of the signal is 3.5 GHz, and the synthetic bandwidth is 320 MHz (for a synthetic wideband signal, β is approximately equal to the synthetic wideband of the signal), it is required that the SNR of the echo should be greater than 36.3 dB in order to correctly unwrap the phase ambiguity.

If the SNR does not satisfy (16), it may increase the accuracy of the envelope range measurement through track filtering, which is equivalent to conducting non-coherent accumulation for the existing echo information, significantly reducing the requirements on single-frame echo SNR.

Moreover, we can also take advantage of the smoothness and slow variation of the range for the target (maneuvering targets waived) to carry through the phase unwrapping for the phase increment of adjacent frames. Then, we can determine the ambiguous phase results with the same ambiguity number to convert the independent ambiguity unwrapping of single-frame data into simultaneous ambiguity unwrapping of multi-frame data. Thus, we are capable of combining all envelope range measurement values during the

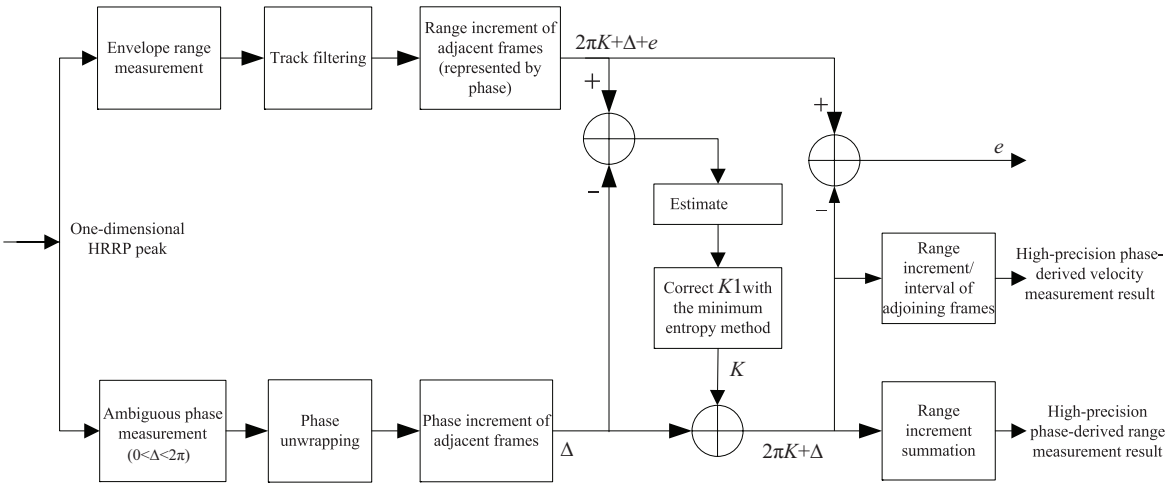

Figure 3 Block diagram for the implementation of high-precision phase-derived range and velocity measurements.

unwrapping of the phase ambiguity. Therefore, it is possible to further reduce the requirements on the envelope range measurement. In the case of defining the minimum average ranging error as the criteria to unwrap the range ambiguity, we simply require that the average envelope range measurement error is less than $\lambda/4$. The premise of the phase unwrapping process is that the change in the range increment of the range profiles for adjacent frames (i.e., acceleration) is not greater than $\lambda/[4(MNT_r)^2]$. As a general rule, the acceleration values of the target are relatively small and satisfy the constraints.

If the SNR is very low, it is very difficult to achieve the range measurement accuracy of $\lambda/4$ after track smoothing; hence, we may use the minimum entropy method to correct the unwrapping of the phase ambiguity results. If the derived range ambiguity of the envelope range measurement result is $K1$, it shall traverse the ambiguity numbers within $K1 \pm L$ (generally, L is defined as 2). Then, the corresponding unwrapping velocity value is used to perform envelope alignment for the echo. By referring to the minimum entropy envelope alignment method for ISAR imaging [17], we assess the entropy of the aligned image, and the ambiguity number corresponding to the minimum entropy will be deemed as the final solution.

3.3.3 *Block diagram for the implementation of high-precision phase-derived range and velocity measurements*

The specific method for the implementation of high-precision phase-derived range and velocity measurements is shown in Figure 3. Because the range measurement result obtained herein is the range increment of adjacent frames, we can gain the phase-derived velocity measurement result with a high accuracy of the target by dividing the range increment with the interval of adjacent frames. The summation of the range increments of adjacent frames provides the phase-derived range measurement result with a high accuracy.

Apart from that, the smoothing filtering of the range increment measurement result after unwrapping ambiguity can further improve the accuracy of the range and velocity measurement.

4 Experimental verification

In this paper, based on the self-developed S-band synthetic wideband PD radar (320 MHz), we have performed the ejection ball experiment, which demonstrated the validity of a high-precision phase-derived range and velocity measurement method applied in point targets. Then, we performed a civil aircraft experiment, which demonstrated the validity of a high-precision phase-derived range and velocity measurement process for complex targets.

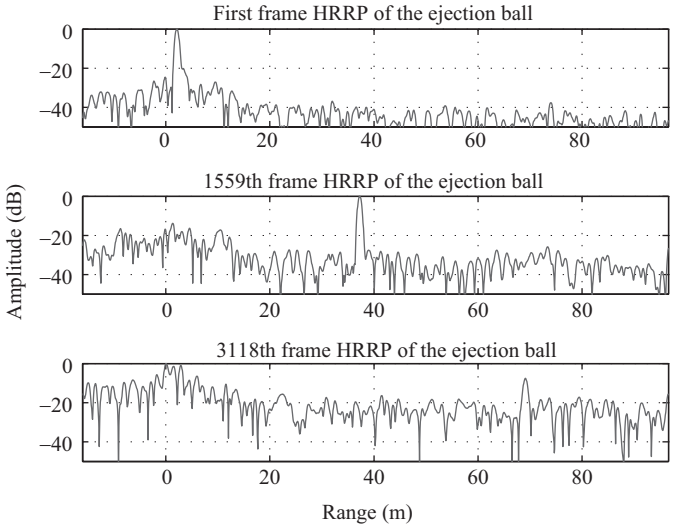

Figure 4 One-dimensional HRRPs of the ejection ball at different moments.

4.1 Ejection ball experiment

Using the radar applied SF signal, the diameter of the ejection ball was just 5 cm, and its RCS was relatively small. The echo was conducted with data processing, as shown in Figure 2, to filter out the clutter and achieve coherent accumulation.

The ejection ball echo was performed for the two-dimensional range-velocity high-resolution imaging process, and then obtained the one-dimensional HRRPs of the velocity dimension where the ejection ball was located. The one-dimensional HRRP of the first, intermediate, and last frames are depicted in Figure 4. As illustrated in Figure 4, the radar recorded the echo data of the ejection ball moving from 2 m to 69 m. When the ejection ball was away from the radar, the SNR of its echo decreased from above 40 dB to approximately 15 dB.

The envelope range measurement result is depicted in Figure 5. Particularly in Figure 5(a), the blue curve shows the envelope range measurement result, and the red curve shows its least-squares track filtering result, while the difference in the results before and after track filtering is deemed as the envelope range measurement fluctuation error, and it is inferred that the RMS fluctuation error of the envelope range measurement is 28.3 mm.

The track filtering result in Figure 5(a) is used to unwrap the phase ambiguity. The measurement result is depicted in Figure 6. The blue curve shows the range increment measured result of adjacent frames, and the red curve shows the fitting result, as the existence of a large curvature in the blue curve. Thus, it adopts segmented fitting pattern; the difference between the measured result and its fitting result is recognized as the phase-derived range measurement fluctuation error, as shown in Figure 6(b). When the SNR is greater than 25 dB, the RMS fluctuation error of the phase-derived range measurement result is 0.05 mm. When the SNR is greater than 40 dB, the RMS fluctuation error of the phase-derived range measurement result is 0.28 mm. In other words, when the SNR gradually decreased from above 40 dB to 15 dB, the phase-derived range measurement fluctuation error gradually increased; however, its RMS fluctuation error is always controlled in the level of submillimeter, which is consistent with the accuracy of the theoretical phase-derived range measurement result.

The range increment measurement result of adjacent frames is divided by the interval of adjacent frames, which can measure the target velocity, as shown in Figure 7(a), wherein, the velocity ascent segment reveals that within a short period of time after the ejection of the ball, the change in the perspective of the ball relative to the radar is relatively large. Thus, the radial velocity changes accordingly; while the deceleration segment is mainly due to the effect of air resistance, the ball velocity is reduced; similarly, the phase-derived velocity measurement error is available to be derived, as depicted in Figure 7(b). The Figure 7(b) shows that the RMS fluctuation error of the phase-derived velocity measurement has grad-

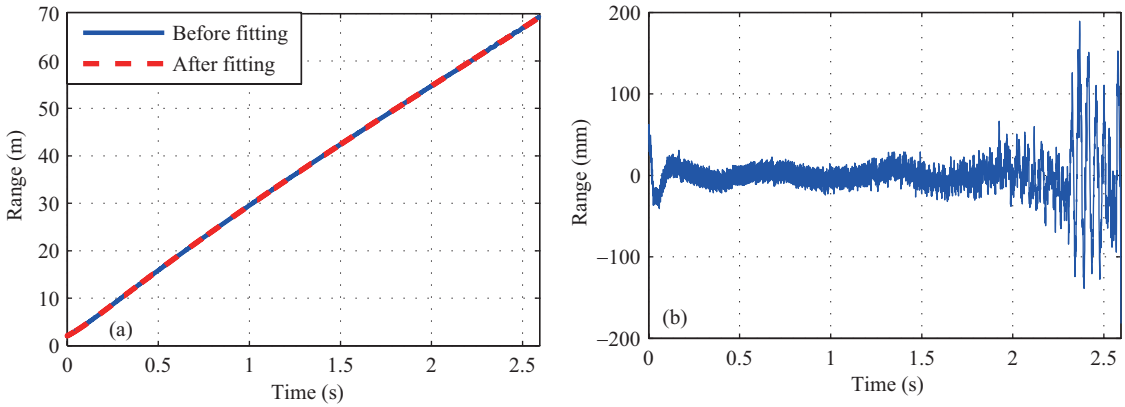

Figure 5 Schematic diagram of the envelope range measurement result and error. (a) Envelope range measurement result; (b) envelope range measurement error.

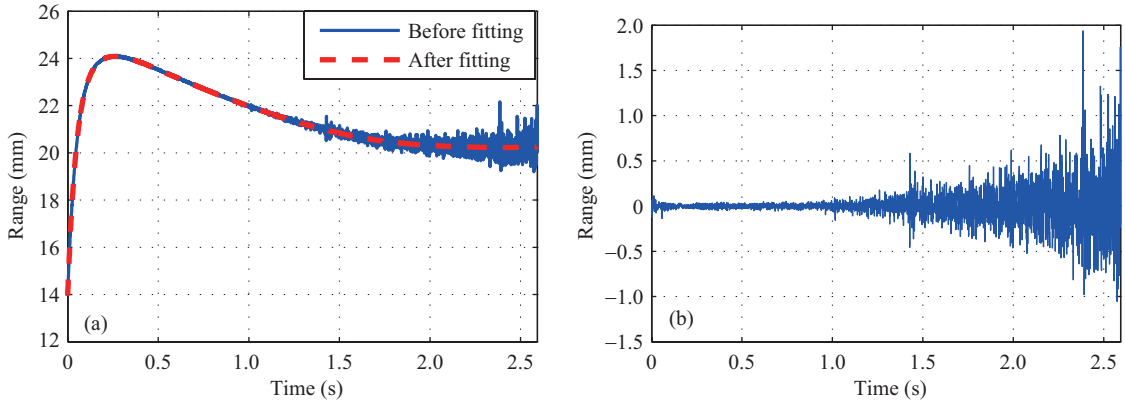

Figure 6 Schematic diagram for the range increment measurement result and measurement error of adjacent frames. (a) Phase-derived range measurement result; (b) phase-derived range measurement error.

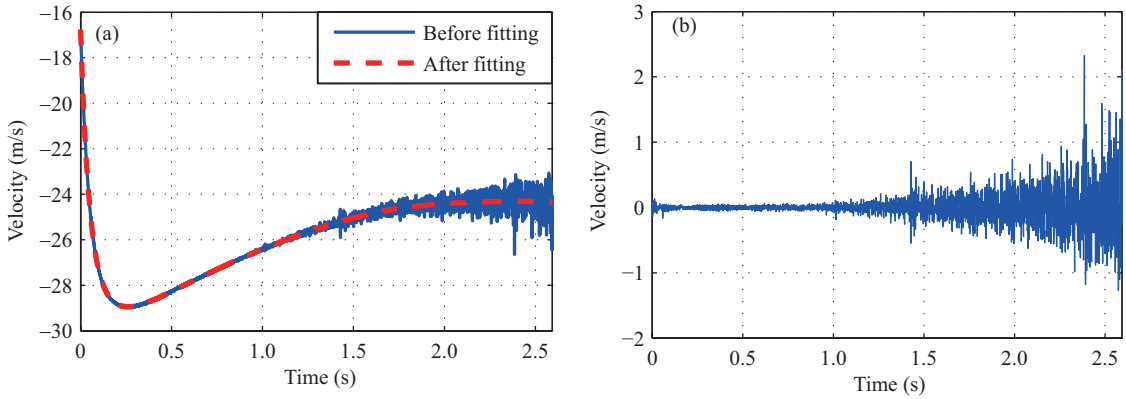

Figure 7 Schematic diagram of the phase-derived velocity measurement results. (a) Phase-derived velocity measurement result; (b) phase-derived velocity measurement error.

ually modified from the level of centimeter/second to submillimeter/second. The summation of range increments for adjacent frames can recover the target trajectory from the phase-derived range measurement.

4.2 Civil aircraft experiment based on dominant scatterer

The radar utilized a PCSF signal to record aircraft landing echoes. In the range segment where the aircraft echo is free from clutter, the pulse width of the signal is relatively large, and the SNR of the

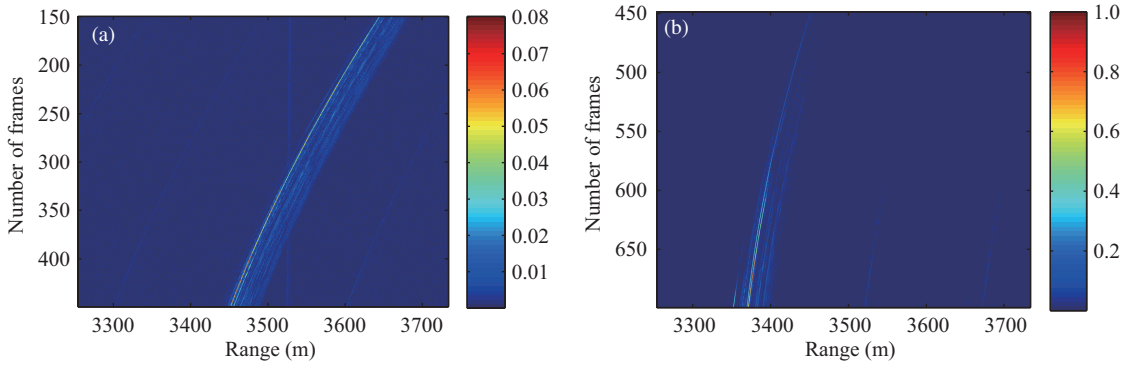

Figure 8 One-dimensional HRRPs of the aircraft over time. (a) 150–500 frames; (b) 500–700 frames.

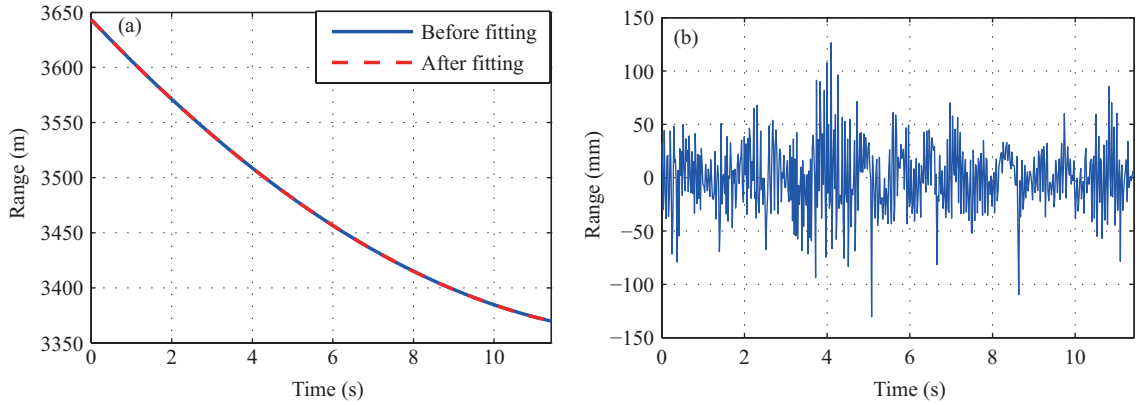

Figure 9 Schematic diagram of the envelope range measurement results and error. (a) Envelope range measurement results; (b) envelope range measurement error.

echo is relatively high. It is able to perform one-dimensional HRRP directly, while the high-precision phase-derived range and velocity measurements based on the one-dimensional HRRP have the identical process flow as mentioned above.

In accordance with the analysis of the 150–700 frame echo data, the one-dimensional HRRPs of the aircraft are illustrated in Figure 8. Because of the limited dynamic range of the image displayed, the one-dimensional HRRPs of the aircraft for 150–700 frames over time are depicted separately. The Figure 8 shows that there is a dominant scatterer, which is the aircraft nose in line with the ISAR imaging results. The following section will discuss the high-precision phase-derived range and velocity measurement results.

The envelope range measurement result for the echo of the aircraft nose is depicted in Figure 9, and the meanings of various curves are identical with those of Figure 6. The statistics suggests that the RMS fluctuation error of the envelope range measurement result is 31.7 mm.

Similar to Subsection 4.1, we were able to obtain the phase-derived velocity measurement result as shown in Figure 10, and the statistics suggests that the RMS error of the phase-derived range measurement result is 1.15 mm, while the RMS fluctuation error of the phase-derived velocity measurement result is 5.51 cm/s.

The summation of the range increments of adjacent frames can recover the target trajectory from the phase-derived range measurement.

5 Conclusion

In this paper, experiments have commendably validated the correctness and feasibility of the phase-derived range and velocity measurement technology. The approach, based on synthetic wideband PD radar, could not only effectively achieve coherent accumulation, but could also inhibit static and low-speed

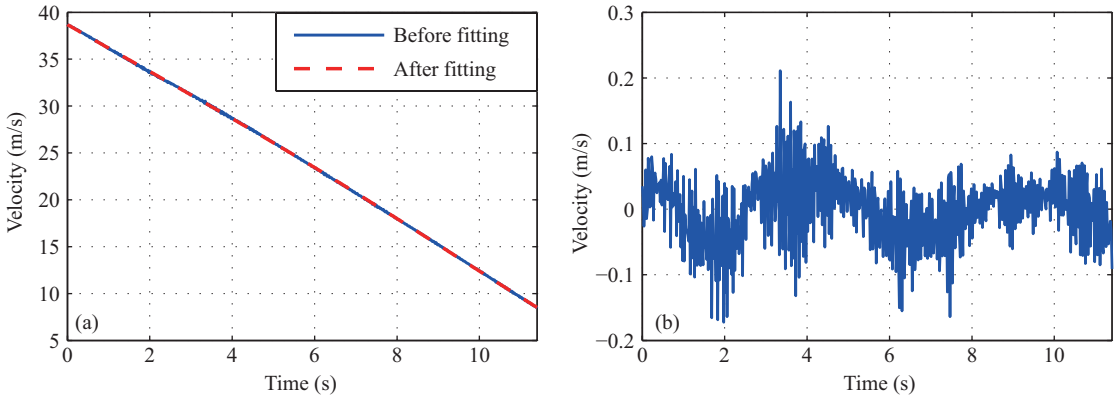

Figure 10 Phase-derived velocity measurement results. (a) Phase-derived velocity measurement results; (b) phase-derived velocity measurement error.

clutter. Combined with the proposed method, it is able to correctly unwrap the phase ambiguity at low SNR and achieve the phase-derived range and velocity measurements with high precision. In particular, the accuracy of the phase-derived range measurement reached the level of submillimeter or millimeter, and the accuracy of the phase-derived velocity measurement reached the level of centimeter/second or submillimeter/second. In addition, the experimental results also show that this method is suitable for point targets and appropriate for complex targets with dominant scatterers.

In the wake of developments in radar technology, we desperately need to improve the capabilities of radar to finely depict target motion. Thus, the high-precision phase-derived range and velocity measurement technology will become a hot spot of future research and will soon be applied to micromotion measurements and target recognition.

Acknowledgements This work was supported by 111 Project of China (Grant No. B14010) and National Natural Science Foundation of China (Grant No. 61301189).

Conflict of interest The authors declare that they have no conflict of interest.

References

1 Liu H B, Lu J D. Target motion compensation algorithm based on Keystone transform for wideband pulse Doppler radar. Trans Beijing Inst Tech, 2012, 32: 625–630
2 Long T, Ren L X. HPRF pulse Doppler stepped frequency radar. Sci China Ser F-Inf Sci, 2009, 52: 883–893
3 Bao Y X. Signal processing algorithms in stepped frequency wideband radar. Dissertation for PH.D. Degree. Beijing: Beijing Institute of Technology, 2010. 40–106
4 Gao W B, Ding Z G, Zhu D L, et al. Improved spectrum reconstruction technique based on chirp rate modulation in stepped-frequency SAR. Sci China Inf Sci, 2015, 58: 102308
5 Jin K, Wang W D, Wang D J. The study on a new radar waveform (PCSF) with high range resolution. J Univ Sci Tech China, 2006, 36: 137–142
6 Steudel F. An Improved Process for Phase-Derived-Range Measurements. World Intellectual Property Organization Patent, 1651978, 2005-2-24
7 Steudel F. Process for Phase-Derived-Range Measurements. U.S. Patent, 7046190, 2005-2-10
8 Skolnik M I. Introduction to Radar Systems. 3rd ed. Beijing: Publishing House of Electronics Industry, 2007. 313–402
9 Liu Y, Hou Q K, Xu S Y, et al. System distortion analysis and compensation of DIFS signals for wideband imaging radar. Sci China Inf Sci, 2015, 58: 020304
10 Wang H F, Ren L X. Velocity estimation of moving targets with stepped-frequency radar based on Doppler frequency difference. J Beijing Inst Tech, 2014, 23: 78–82
11 Li L. Theory and implementation of stepped-frequency radar signal processing. Dissertation for PH.D. Degree. Beijing:

Beijing Institute of Technology, 2010. 55–68

12 Tian J, Cui W, Shen Q, et al. High-speed maneuvering target detection approach based on joint RFT and keystone transform. Sci China Inf Sci, 2013, 56: 062309

13 Gao M G, Zhou D Y, Mao E K. A method of digital moving target track based on waveform analysis. Chinese J Electron, 1998, 26: 112–114

14 Liu Y X, Zhu D K, Li X, et al. Micromotion characteristic acquisition based on wideband radar phase. IEEE Trans Geosci Remote Sens, 2014, 52: 3650–3657

15 Bao Y X, Ren L X, He P K, et al. Velocity measurement and compensation method based on range profile cross-correlation in stepped-frequency radar. Syst Eng Electron, 2008, 30: 2112–2115

16 Li L, Ren L X, Mao E K, et al. Accurate velocity measurement of range profile cross correlation in stepped-frequency signal. Trans Beijing Inst Tech, 2011, 31: 708–712

17 Wang G Y, Bao Z. The minimum entropy criterion of range alignment in ISAR motion compensation. In: Proceedings of Conference Radar, Edinburgh, 1997. 14–16